Interference with the Development of Early Generated Neocortex Results in Disruption of Radial Glia and Abnormal Formation of Neocortical Layers

Stephen C. Noctor[1], Sidney L. Palmer[2], Thomas Hasling[2] and Sharon L. Juliano[1,2]

[1]Program in Neuroscience and [2]Department of Anatomy & Cell Biology, USUHS, Bethesda, MD 20814, USA

Early generated layers of neocortex are important factors in forming the subsequent architecture of the cerebral cortex. To further explore the role of early generated cortex, we disrupted formation of an early generated cohort of cells by intraperitoneal injections of the mitotic inhibitor methylazoxymethanol (MAM) into pregnant ferrets timed to coincide with generation of subplate neurons in the ventricular zone. Our studies demonstrate that if early development of the neocortex is interrupted by injection of MAM during embryogenesis (on embryonic day 24 or 28; E24 or E28), a distinct laminar pattern fails to form properly in the parietal cortex. A reduced number of MAP2-positive cells were observed in the region of the subplate when compared with the number of MAP2-positive cells found in normal animals. Interference with the superficial neocortical layers that form later during development (on embryonic day 33) by appropriately timed MAM injections does not result in a severely disrupted laminar pattern. The interrupted laminar pattern that arises after early MAM injections coincides with distorted radial glial cells (identified by immunoreactivity to the intermediate filament protein, vimentin), which occur after early, but not late, MAM injections. Further analysis suggests that interference with early development of neocortex leads to premature differentiation of radial glial cells into astrocytes, as demonstrated by the presence of glial fibrillary acidic protein (GFAP). Experiments involving injections of the thymidine analog, bromodeoxyuridine (BRDU), demonstrated that 4 days after E24 MAM injection cells are generated and migrate into the thin cortical plate. By E38, however, cells continue to be generated in animals treated with MAM on E24 but do not reach their normal positions in the cortical plate. In addition, immunoreactivity using the CR50 antibody, which identifies presumptive Cajal–Retzius cells present in layer 1, demonstrates that the CR50-positive cells, normally precisely located in the outer portion of layer 1, are distributed in disarray throughout the thickness of the neocortex and intermediate zone in early MAM-treated animals, but not in those treated with MAM injections later during gestation. These findings are consistent with the idea that early generated layers are important in providing factors that maintain the environment necessary for subsequent neuronal migration and formation of neocortical layers.

Introduction

The layers generated during early cortical neogenesis may play a key role in further neocortical development. Of the early born layers, the subplate participates in a number of processes that help the cortical architecture to mature. Its neurons extend pioneering axons centrifugally to the thalamus to guide thalamic afferents into the cortex (McConnell *et al.*, 1989; De Carlos and O'Leary, 1992; Erzurumlu and Jhaveri, 1992); subplate neurons participate in early functional circuits that link thalamic afferents with the subplate and the subplate with layer 4 (see Allendoerfer and Shatz, 1994 for review). In visual cortex, the subplate also appears to be important in directing thalamic afferents into ocular dominance columns, since deletion of subplate neurons in neonatal cats prevents segregation of geniculocortical afferents into distinct clusters (Ghosh *et al.*, 1990; Ghosh and Shatz, 1992a,b, 1994).

It is not clear whether the early generated layers, including the subplate and deep neocortical layers, are important to subsequent laminar formation and migration of neurons into the cortex. A genetic model of distorted cortical layer formation, the *reeler* mouse, suggests that layers form without certain positional cues, although in a misplaced manner. In *reeler* mice, the preplate, which normally splits and allows the subsequent layers to form between its deepest element (the subplate) and its most superficial element (layer 1), does not divide and the normally occurring inside-out pattern of laminar genesis does not take place (Caviness and Rakic, 1978). Instead, cortical layers build up beneath each other in an upside-down fashion and the subplate remains superficial, towards the pia. Even in *reeler* mice, however, the subplate appears to play an important role in cortical development, since axons from the thalamus grow directly into the superficially located subplate and then downward into layer 4, the normal recipient layer from the thalamus (Frost and Caviness, 1980; Caviness and Frost, 1983; Molnar and Blakemore, 1995).

One way to test the impact of early generated cortical layers on later-born layers is to investigate the maturation of cerebral cortex in animals that continue to develop after interference with the early produced layers. Other studies have evaluated the impact of subplate deletion on subsequent formation of cortical architecture by removing the subplate postnatally, after a substantial portion of cortex has already formed (Ghosh *et al.*, 1990; Ghosh and Shatz, 1992a, 1994). Although this method is highly useful and important in evaluating structures that mature later in cortical development, such as thalamocortical distribution, it does not allow assessment of the impact of the subplate on earlier events. To test the role of early generated layers on subsequent events we conducted an experimental series in which we disrupted the development of the subplate and/or deeper cortical layers by *in utero* injection of methylazoxymethanol acetate (MAM) into pregnant ferrets on appropriate gestational days. MAM is a toxin that prevents cells from dividing for a short period of time, thereby effectively preventing the birth of a given population of cells that would normally divide at the time of the injection (Matsumoto and Higa, 1966; Zedeck *et al.*, 1970; Matsumoto *et al.*, 1972; Johnston *et al.*, 1979; Cattabeni and Di Luca, 1997). Using this method can therefore interfere with the formation of a specific layer of neocortex (Johnston and Coyle, 1979; Jones *et al.*, 1982; Virgili *et al.*, 1988; Fasolo *et al.*, 1992). Our results indicate that MAM injections early during cortical development result in severely disrupted cortex together with dramatic alteration of radial glial and Cajal–Retzius cells, while later injections of MAM, timed to disrupt layer 4 development, cause more subtle

cortical changes and do not produce dramatic alterations in cortical structure or radial glia.

Materials and Methods

To determine the effect of interrupting corticogenesis early during the birth of cortical cells or later during their genesis, we injected MAM into pregnant ferrets. The injections were made either early during corticogenesis on embryonic day 24 (E24) or E28 or later during corticogenesis on E33. The early MAM injections disrupted the development of the subplate or deep portions of layer 6 (for the E28 injection) of ferret somatosensory cortex. The E33 injections interfered with layer 4 development. These dates were decided by an earlier study that determined the birthdates of cells populating ferret somatosensory cortex using bromodeoxyuridine (BRDU), an analog of thymidine (Noctor *et al.*, 1997). A number of animals received injections of BRDU 0–14 days after MAM injections to determine the viability and migration of cells after MAM treatment.

Several techniques were used to assess the effect of MAM treatment on the development and architecture of the parietal cortex; all further analyses were made within 1 week of birth (i.e. by P7) except for BRDU immunohistochemistry (see below). The architecture was assessed using standard histological techniques including Nissl stain and immunoreactivity for various markers specific for neurons and glia, including antibodies directed against MAP2, Cajal–Retzius cells (CR50), vimentin and glial fibrillary acidic protein (GFAP). We also used injections of anatomical tracers into live slices to study the architecture of the MAM-treated brains, since previous studies revealed that slice preparations were useful in this regard, particularly for evaluating the status of radial glial cells (Juliano *et al.*, 1996). Additional animals in each group (i.e. normal, early MAM-treated or late MAM-treated) were reacted for immunoreactivity against BRDU. Several animals in the late (E33) MAM-treated group were reacted for BRDU when they reached maturity (after 1 month). Western blots were conducted on tissue obtained from P0 animals treated with MAM on E24 and from normal P0 kits to test for the presence of GFAP. In two pregnant animals, MAM was injected on E24 and the embryos evaluated at E27 and E35 to determine the effect of MAM at shorter times after the *in utero* injection.

All assessments were made in the parietal cortex before P7. The only exceptions to this were cases of several animals that received BRDU after E33 MAM treatment, in which the brains were analyzed at 1–2 months of age. Before P7, ferret brains are immature and morphological landmarks are not clearly developed. To ensure that we assessed comparable regions across animals, a coronal block of neocortex was selected in each brain corresponding to landmarks that correlate with parietal cortex in the adult ferret. This block included the region immediately posterior to the anterior commissure and immediately anterior to the thalamus. Within each section, only regions in the dorsolateral portion of the neocortex were used for analysis; this restriction excluded the most medial and lateral portions of cortex (Fig. 1). Although it is not possible to judge accurately cortical regions by cytoarchitecture before P7 in ferret, enough landmarks are present to assign injection sites to lateral portions of parietal cortex, which correspond to the forelimb representation in area 3b (Juliano *et al.*, 1996; Noctor *et al.*, 1997; McLaughlin *et al.*, 1998). In addition, for the animals treated with MAM early during corticogenesis the brains are even smaller than normal or E33 MAM-treated brains, with fewer external landmarks, making the certainty of the cortical site chosen difficult. The internal regions chosen to identify the desired cortical region were present in the brains of all groups, however, so it is likely that similar sites were assessed under all treatment conditions.

Injections

Timed pregnant ferrets were obtained from Marshal Farms (New Rose, NY). MAM injections were made into pregnant ferrets on appropriate days of gestation. Ferrets were anesthetized with halothane (2%) and the MAM injected i.p.; each ferret received 12 mg/kg of MAM (Sigma) dissolved in saline. BRDU injections were made into pregnant ferrets on different embryonic days after MAM injections on E24 or E33. The injections were made i.p. under halothane anesthesia (2%) and delivered 60 mg/kg of BRDU (Sigma) dissolved in saline with 0.007 N NaOH. After the kits were born, BRDU-labeled cells were revealed using standard immunohistochemical techniques (see below). In this set of experiments, kits were examined from P0 to P7, except for several E33 MAM-treated animals that received BRDU injections, which were assessed on P28 and P42, when the laminar pattern of the somatosensory cortex is histologically mature (Juliano *et al.*, 1996). This allowed us to assess the final position of BRDU-positive cells in mature cortex. On the appropriate date, each kit received an i.p. injection of sodium pentobarbital (50 mg/kg) and, when insensitive to pain, was perfused through the heart with saline followed by 4% paraformaldehyde in 0.1 M phosphate buffer. The brains were removed and sunk in 10% and then 20% sucrose in phosphate buffer at 4°C and then frozen in isopentane at –35°C and kept in a freezer at –70°C, until processed as below. In most instances, when the brains were cut, alternate sections were saved for either BRDU, CR50, MAP2, GFAP or vimentin immunohistochemistry, or Nissl staining (see below).

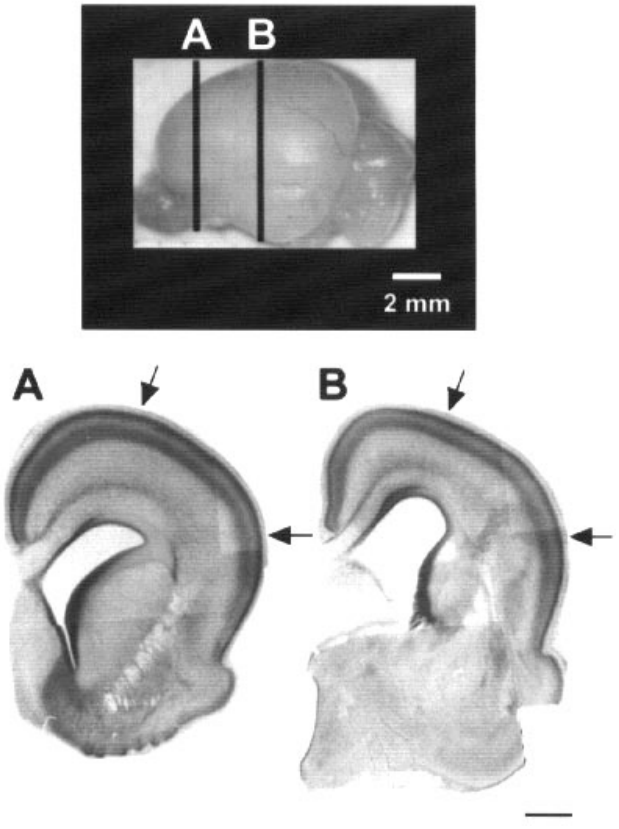

Figure 1. On top is a photograph of a P0 ferret brain and below are sections taken at the levels indicated by the lines A and B. On the individual sections (*A*, *B*) are arrows bounding the region studied within each section; this location corresponds to the developing somatosensory cortex. The location identified in each slice or section was within lines drawn at 30° and 90° from vertical.

Immunohistochemistry

The brains were cut in a cryostat at –16°C at 30 μm thickness. Antibodies against vimentin (Boehringer Mannheim, anti-vimentin, clone V9), MAP2 (Boehringer Mannheim, anti-MAP2), GFAP (Boehringer Mannheim, anti-GFAP) or CR50 (a generous gift from K. Nakajima, RIKEN, Japan and M. Ogawa, Kochi Medical School, Japan) were applied to the sections after blocking with 10% normal horse serum, 0.2% gelatin plus 0.1% Triton X (Sigma). After 12 h incubation with the primary antibody (diluted 1:4 with 2% normal horse serum and 0.1% Triton X), the sections were rinsed with 0.1 M PBS, pH 7.4, and incubated in the secondary antibody (Vector, antimouse IgG conjugated to fluorescein or Texas Red at 1:100 in 2% normal horse serum and 0.1% Triton X or Vector Vectastain Elite ABC kit) for 2 h. At this point, the resulting label was visualized with fluorescent microscopy or using a Vector VIP peroxidase substrate kit. Control sections received no primary antibody.

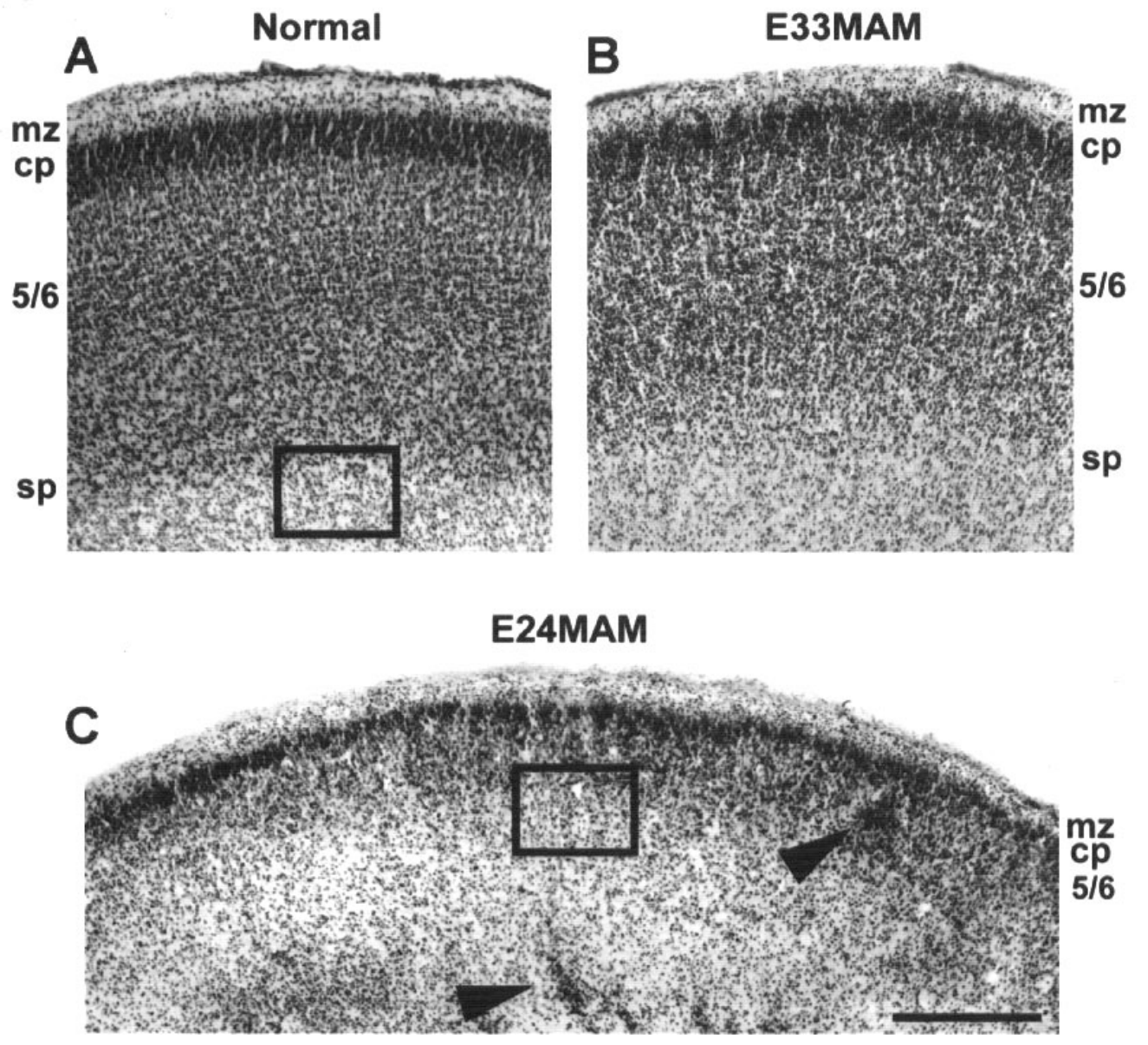

Figure 2. Nissl-stained sections of ferret somatosensory cortex cut in the coronal plane at P1. (*A*) is taken from a normal kit, (*B*) is taken from a kit that received a dose of MAM at E33, (*C*) is from a kit that received a dose of MAM at E24. In the newborn ferret somatosensory cortex, layers are poorly formed; visible in (*A*) and (*B*) are the dense cortical plate (CP), the poorly formed layers 5 and 6, and the subplate (SP). In (*C*), taken from a kit treated with MAM at E24, cortical layers fail to form and a thin sheet of cells is present in place of the normally layered cortex. Arrows point to ectopic clusters of cells that form. Layer 1 is somewhat thinner toward the right edge of the image. The rectangles in (*A*) and (*C*) indicate the regions chosen for analysis of MAP2-IR neurons in Figure 9. Scale = 250 μm.

For BRDU immunohistochemistry, sections were treated with 95% ethanol and 5% acetic acid for 30 min, 1 mg/ml pepsin (Sigma) in 2 N HCl for 1 h at 37°C, then rinsed in 0.1 M PBS, pH 8.5. Sections were incubated in the primary antibody (anti-BRDU Boeringer-Mannheim; 1:20 with 2% normal horse serum and 0.1% Triton X-100) at 4°C overnight. The following day, sections were rinsed in 0.1 M PBS, pH 7.4, and then incubated in the secondary antibody (Vector Vectastain Elite ABC kit) for 1 h, rinsed in 0.1 M PBS, pH7.4, and finally incubated in ABC for 1 h. The immunoreaction product was visualized with DAB.

Immunohistochemistry Quantification

In order to determine relative numbers of MAP2-positive neurons in the subplate region of normal and E24 MAM-treated animals, MAP2-immunoreactive (IR) cells were counted in a defined region (see Fig. 2). Cells were sampled in a 200 × 150 μm sector of five sections through the subplate region of the somatosensory cortex in each animal (see rectangles in Fig. 2*A*,*C*). Three animals in each group were counted; the groups include (i) normal BRDU-IR, (ii) normal MAP2-IR and (iii) E24 MAM-treated MAP2-IR. A mean value was determined for each animal and used in a two-tailed *t*-test to determine the relative number of labeled cells in each group.

To determine the approximate number of CR50-IR cells in normal and E24 MAM-treated animals, CR50-positive cells were counted by choosing evenly spaced sections between the rostrum and splenium of the corpus callosum in both animals; all clearly labeled CR50-IR cells were counted. The most medial and most lateral portions of cortex were excluded (see Fig. 1). The number of cells was assessed using the Abercrombie correction (1946), recently discussed by Guillery and Herrup (1997). The following equation was applied: $N = n[T/(T + D)]$, where N corresponds to the 'true' number, n is the estimated number, T is the section thickness and D is the mean diameter of the objects measured perpendicular to the section plane.

Acute Slices

Live slices were prepared from three groups of animals ranging in age from P0 to P7 (day of birth is considered to be P0): (i) normal kits (n = 12), (ii) kits whose mothers received MAM treatment on E24 or 28 (early group, n = 21), and (iii) kits whose mothers received MAM treatment on E33 (late group, n = 25). Slices were prepared at P0–7 by injecting each kit with 50 mg/kg pentobarbital i.p.; the brains were then removed. During brain removal, ice-cold artificial CSF (containing in mM: NaCl 124, $NaHCO_3$ 26, NaH_2PO_4 1.2, KCl 3.2, $MgSO_4$ 1.2, $CaCl_2$ 2.4, glucose 10) was perfused often onto the brain until it was blocked and cut. The somatosensory cortex was cut into 400 μm thick coronal slices using a tissue chopper and placed directly in an oxygenated chamber perfused with artificial CSF. A mixture of oxygen (95%) and carbon dioxide (5%) was bubbled through polyethylene tubing from below into the chamber near the stage that held the slices. The same gas mixture was also bubbled into the CSF that perfused the slices from below. At this point, injections of fluorescent dextrans (dextran fluorescein or fluororuby, Molecular Probes, Inc.) were made iontophoretically (3 μA, alternating positive current for 4 min) through pipettes with a tip thickness of 10–15 μm. The injections were made at a depth of 200 μm into the approximate center of the slice. The injection sites were all made in the dorsal and lateral portions of parietal cortex (presumptive somatosensory cortex) or into immediately underlying structures including the ventricular zone (VZ) or into the intermediate zone (IZ). The slices remained in the chamber for 5–8 h to allow for transport. The slices were maintained at room temperature, as described previously (Juliano *et al.*, 1996). We determined in earlier studies that unhealthy slices do not transport dextran tracers (Juliano *et al.*, 1996). Several other studies report using similar methods for maintaining acute slices (e.g. Blanton *et al.*, 1989; Yuste *et al.*, 1995; Wiser and Calloway, 1996; Flint *et al.*, 1997; Calloway, 1998; Kandler and Katz, 1998). In addition, during most sessions, representative slices were removed and used for Ca^{2+} imaging. Although these Ca^{2+}-imaged sections were used for other purposes, they also served as a good control to measure the health and viability of the slices, which were found to display calcium transients for at least the length of time the slices were maintained in the chamber. In most instances, the slices were fixed overnight in 4% buffered paraformaldehyde with 10% sucrose in phosphate buffer, then they were sunk in 20% sucrose in phosphate buffer. After this, the slices were further sectioned at 40 μm thickness using a freezing microtome. The label resulting from the dextran injections was visualized using either conventional fluorescent or confocal microscopy (BioRad, MRC 600). Many injections were drawn from the digitized confocal images (×20) to visualize further details across several sections using the Neurolucida reconstruction program (MicroBrightField, Inc.).

Western blots

Tissue samples were obtained from either normal or E24 MAM-treated P0 kits; regions of the telencephalon were dissected that included the cortex, the IZ and the VZ. The brain pieces were homogenized in 10 mM Tris buffer, pH 7.6; total soluble protein was determined (with the Bio-Rad protein detection kit). The samples and sample buffer were boiled and loaded (100 μg total protein) onto 12% acrylamide gels alongside low molecular weight non-stain markers. A Bradford assay was performed to ensure that the total protein concentration in each sample was the same. After running the gels, they were transferred to a Hybond-ECL membrane (Bio-Rad). To detect GFAP, an anti-GFAP antibody was used at 1:1000 and visualized using an ECL Western blotting analysis system (Amersham) and exposed to Hyperfilm-ECL.

Results

General Organization of Parietal Cortex in Normal and MAM-treated Animals

The total number of animals for all experimental conditions and for acute slice injections can be seen in Tables 1 and 2. The cytoarchitecture of the somatosensory cortex at P0–7 in normal animals consists of a dense cortical plate (i.e. developing and differentiating upper and middle layers of cerebral cortex) and a poorly formed layer 5 and 6; the subplate is also observable. At this age, layer 4 cannot be distinguished from the other layers that make up the dense cortical plate (Fig. 2*A*). In this paper we use the term 'cortical plate' to refer to the full thickness of the cortex including layers 2–6 (if distinguishable); 'dense cortical plate' refers to the undifferentiated layers 2–4 observed in ferret somatosensory cortex during P0–7. The border between layer 6 and the subplate or the white matter (in older brains) is easily distinguishable; layer 5 cannot always be distinguished from layer 6 before 1 week of age.

Table 1
Total number of animals used for all analyses

E24 or E28 MAM kits	E33-34 MAM kits	Normal kits	E24 MAM embryos at E27 or E35
21	25	12	8
Number of dams			
7	8	8	2

Table 2
Numbers of animals and acute slices used for injections. Multiple slices were obtained from each kit, multiple injections were made in each slice, within the defined region of interest.

	Kits	Slices	Injections
E24, 28 MAM	8	60	181
E33, 34 MAM	9	58	172
Normal	6	30	124

In slices obtained from animals treated with MAM on E33 (the late group, layer 4 disruption) the architecture of the cortex looked similar to that in normal animals, i.e. poorly formed layers 5 and 6 were present, as well as a dense cortical plate. The subplate is also substantial and present (Fig. 2*B*). Measurements of the thickness of the cortex were made from the external limit of layer 1 (i.e. the pia) to the border between layer 6 and the subplate. This border was identified by a dramatic decrease in the density of cells. All measurements of cortical thickness occurred in the middle portion of the region used for analysis (Fig. 1). The cortex is slightly thinner than normal in E33 MAM-treated animals, with a mean value of 380 μm (n = 5) in thickness, compared with mean value of 411 μm in thickness for the normal (n = 4); these values were not significantly different (two-sample t-test). Although the later MAM injection (E33) had little obvious early effect on newborn kits, these injections result in a poorly formed layer 4 when kits are observed at cortical maturity (Noctor *et al.*, 1995).

In the group of animals that received early MAM, two dates of injection were used: E24 or E28. Injections on either of these days resulted in severely disorganized cortical architecture. The brains of these animals were significantly smaller than their normal counterparts. This was tested by measuring the cross sectional area in single sections at the level of the anterior commissure in five normal and five early MAM-treated animals. The cross sectional area at this rostrocaudal level was significantly smaller in the MAM-treated group (7.41 mm^2 in E24 MAM-treated compared to 16.28 mm^2 in normal animals; $P \leq 0.001$, two-sample t-test). The cortical plate was very thin, with a mean value of 103 μm in thickness from the pia to the cellular border with the white matter compared with a mean value of 411 μm in cortical thickness in normal animals at P1. Although

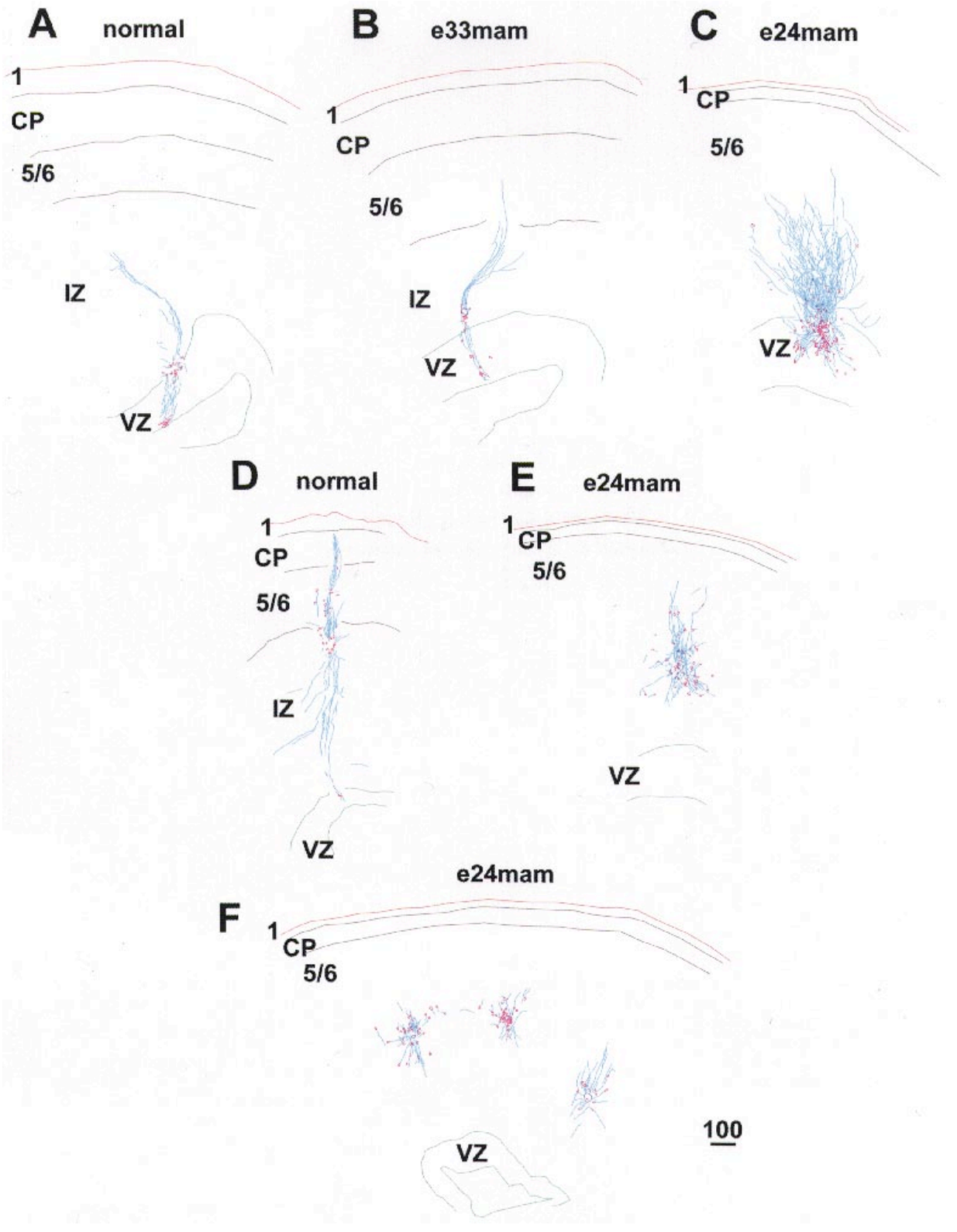

Figure 3. Label resulting from injections of fluorescent-tagged dextrans in live slices of ferret somatosensory cortex taken at P1. In (*A–C*) Injections were made in the ventricular zone (VZ) of the slices; in the normal animal (*A*), the label extends in a column-like array, reaching from the ventricular edge toward the cortical surface. The label is comprised of radial glial cells and migrating neurons. The injection illustrated in (*B*) is taken from a kit that received a dose of MAM on E33; the resulting label looks nearly identical to the normal pattern. The drawing in (*C*) is obtained from an animal that received a MAM injection on E24; rather than a precise point-to-point distribution, the label fans out from the injection site and does not head directly toward the pia. (*D*) and (*E*) compare dextran injections in normal (*D*) and E24 MAM-treated animals (*E,F*) that were placed in the intermediate zone (IZ). Shown in (*F*) are drawings of three dextran injections made into the IZ of an acute slice after E24 MAM treatment. Compared with the normal (*D*) or E33 MAM-treated (*B*) slices, injections into the IZ of E24 MAM -treated slices were less radial and labeled fragments of presumptive radial glia that passed through the injection site (*E,F*). The blue color indicates the pattern of processes or fibers; pink indicates a cell body. Identifiable layers of cortex are indicated with numbers. CP, cortical plate. Scale = 100 μm.

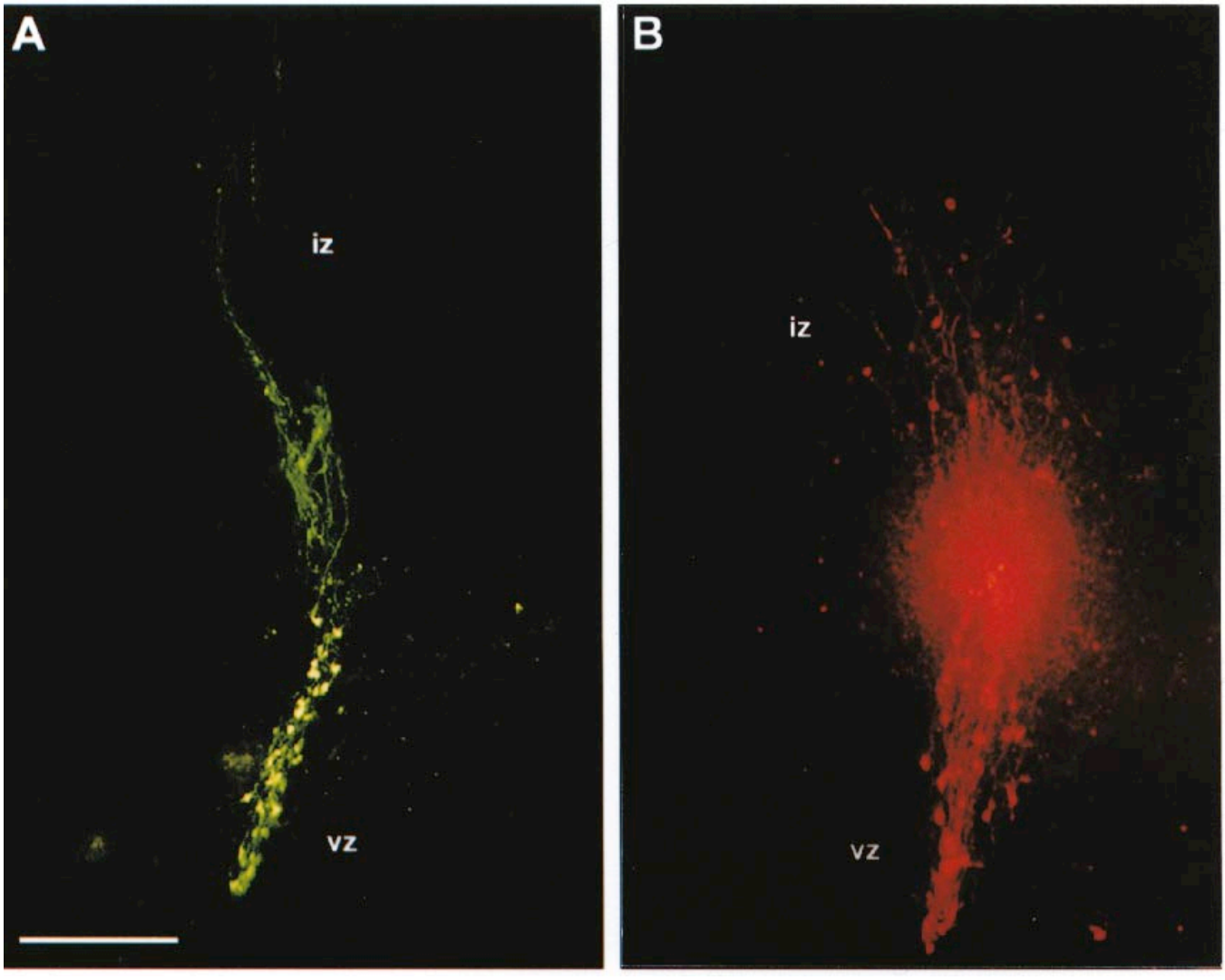

Figure 4. (*A*) Digitized confocal image of a dextran injection into a live slice taken from a P1 normal ferret kit; the label extends in a radial manner toward the cortex. (*B*) A similar injection in a slice obtained from a ferret kit treated with MAM on E24; the resulting label fans out and does not extend directly toward the pia. Scale = 100 μm.

the layers were not clearly defined in these brains, it was always possible to see a sharp decrease in the density of cells that represented the boundary between the cortex and underlying white matter. Neither a clear laminar pattern nor a distinct subplate were found (Fig. 2*C*). Occasional clusters of cells were seen in abnormal arrangements, suggesting that cells were not able to migrate to their proper location (arrowheads in Fig. 2*C*). Layer 1 was present, but varied in thickness and tended to be more normal in appearance towards lateral portions of the parietal cortex. This can be observed in Figure 2*C*, demonstrating a thinning of layer 1 towards the medial aspect of the cortex, on the right side of the image.

Dextran Injections into Acute Slices

In normal animals, injections of fluorescently labeled dextrans into acute live slices resulted in characteristic and precise patterns of label that were strongly radial in nature. This distribution of label occurred after injections into, or near, the VZ. The labeled elements consisted largely of radial glia, which extended long distances from the VZ to the pial surface (Figs 3*A*, 4*A*); neurons migrating to the neocortex were studded along the glial processes (Juliano *et al.*, 1996). Dextran injections into E33 MAM-treated slices resulted in label similar to that in normal animals. This was true whether the injections were placed in the IZ or in the VZ. Presumptive radial glia labeled with the dextrans were distinctly spoke-like, extending from the VZ toward the cortical surface (Fig. 3*B*).

Dextran injections into slices obtained from early MAM-treated animals resulted in a severely disorganized pattern of label, in comparison with the distribution found in normal or E33 MAM-injected animals. After injections into the VZ, rather than a radial flow, the labeled elements formed a fan-like configuration spread over a wide angle, not the point-to-point distribution in normal or E33 MAM-treated animals (Figs 3*C*, 4*B*). The dextran injections into or near the VZ resulted in the distribution of labeled fibers as seen in Figures 3*C* and 4*B*, with the cell bodies labeled in the VZ and the processes extending in disarray into the surrounding white matter. After injections into the IZ, the label was also irregular and spoke-like, and did not form a radial array. These injections, however, resulted in a more fragmented pattern, with the dextran label following several segments of presumptive radial glia (Fig. 3*E*,*F*).

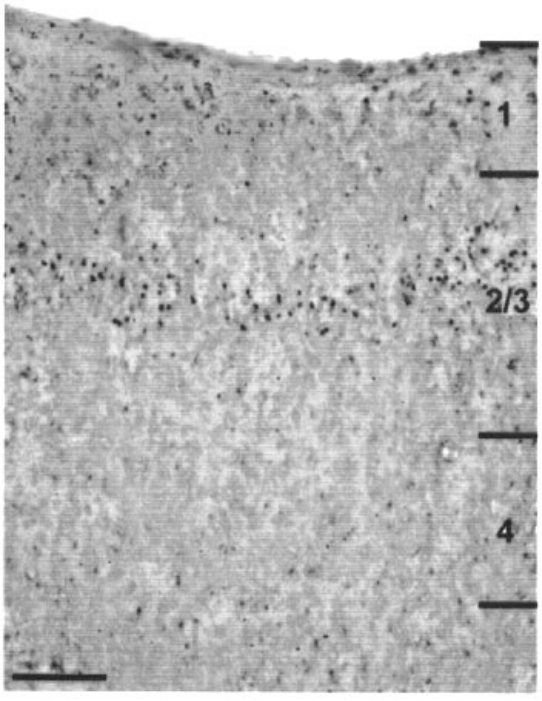

Figure 5. BRDU immunoreactivity in a section taken from a P42 animal that received a MAM injection on E33 and a BRDU injection on E38. The BRDU staining is heavily concentrated in layer 2, the site in which neurons generated on E38 normally reside. Scale = 100 μm.

BRDU Label

Injections of BRDU were made into pregnant ferrets both before and after MAM treatment on E33. In both situations (BRDU delivered E30 and E38) cells were generated and migrated into distinct laminar patterns appropriate for the gestational age of injection. Figure 5 shows an example of BRDU-positive cells observed after an E33 MAM injection followed by BRDU administration on E38. The labeled cells are located in a distinct laminar pattern appropriate for the time of BRDU injection.

BRDU administration after E24 MAM treatment indicated that neurons continued to be born and migrate into the cortex after early MAM injections as well. BRDU injections were delivered on several dates (E24, E28, E30 and E38) in this set of experiments. BRDU injections performed on E24, i.e. at the time of the MAM treatment, resulted in no BRDU-positive cells in the material studied. This observation is logical since MAM disrupts cell division and we would expect no incorporation of BRDU while MAM is active. Data derived after BRDU injections on other dates after the MAM treatment are shown in Figures 6 and 7. Figure 6 contains photomicrographs of neocortical regions containing densely labeled BRDU-positive cells. These were taken after BRDU injections into normal or MAM-treated jills on either E28 (shown on the left, corresponding to the normal birthdate of layer 6) or E38 (shown on the right, corresponding to the normal birthdate of layer 2; Noctor *et al.*, 1997). The inserts in Figure 6 show the overall position of the BRDU-labeled cells. In the two left panels, the BRDU-positive cells reside largely in a distinct band corresponding to layer 6 in the normal animal, whereas in the E24 MAM-treated animal, the labeled cells are distributed throughout the much thinner cortical plate. Labeled cells are also found beneath the cortical plate in the IZ. After a BRDU injection on E38, resulting label in the normal animal occurs throughout the thickness of the cortex and in the IZ, since many of the cells generated on this day have not yet reached their final resting place in layer 2 (Noctor *et al.*, 1997). After E24 MAM treatment and E38 BRDU injection, the BRDU-positive cells are also scattered throughout the IZ, but many fewer of them reach the cortical plate.

These data are quantified in Figure 7. To compare the distribution of labeled cells across similar distances through the cortex in normal and MAM-treated animals, the number of BRDU-positive cells were counted in bins 500 μm wide by 50 μm deep and presented in histograms as the percentage of the total number of cells counted. In the MAM-treated animals, the bins extended into the IZ, as the cortical plate is much thinner in these animals. As indicated above, when BRDU is injected on E28 in the MAM-treated animals, a relatively high percentage of cells are found in the cortical plate (bottom left histogram, layers 5 and 6 cannot be distinguished from the dense cortical plate). After BRDU injection on E38 in the early MAM-treated animals (bottom right histogram) a much lower percentage of cells reach the cortical plate. To test for significant differences between the BRDU distributions in the two MAM-treated conditions, i.e. BRDU injections early (4 days; E28) and late (14 days; E38) after the MAM treatment, we conducted a chi-squared test between the two distributions. This test indicated that the two distributions are significantly different ($P < 0.001$, $\chi^2 = 34.207$, 7 degrees of freedom).

Immunoreactivity

To quantify the effect of early MAM treatment on the number of neurons populating the subplate underlying somatosensory cortex on P0, we studied the number of MAP2-positive cells in the region of the subplate in normal and E24 MAM-treated animals. MAP2 has been identified as a marker for subplate neurons in ferret (Ghosh and Shatz 1992a, 1993). Significantly more MAP2-positive cells were found in normal subplate compared to a similar region in animals treated with MAM at E24 (two-sample *t*-test, Figs 8 and 9). Figure 8 shows MAP2 immunoreactivity in normal (Fig. 8*B*) and E24 MAM-treated (Fig. 8*C*) P0 somatosensory cortex. In both groups, MAP2-labeled cells were observed in the subplate with the characteristic inverted pyramidal shape (Valverde and Facal-Valverde, 1988; Antonini and Shatz, 1990). The regions chosen for analysis are indicated with rectangles in Figure 2*A*,*C*. Figure 8*A* illustrates BRDU-positive cells in the same region on P0 in a normal animal after BRDU injection on E24. Figure 9 demonstrates that in normal animals, there are similar numbers of BRDU-positive cells (after BRDU injection on E24) and MAP2-positive cells in the analyzed subplate region of normal P0 animals. Neurons that reside in the subplate region of ferret somatosensory cortex are born on several days, including E24 (Noctor *et al.* 1997). This analysis provides information about MAP2-positive cells immediately below the cortical plate (i.e. where the subplate normally lies). It does not rule out the possibility that other MAP2-IR cells may be scattered in other locations in the IZ; it only verifies that they are not in the vicinity of the subplate.

Since the spoke-like labeling pattern revealed after dextran injection is largely composed of radial glia, we predicted that the processes of these cells would be specifically disrupted in animals treated with MAM on E24 or E28. The normal pattern of radial glia consists of cell bodies in the VZ, with processes that extend toward the pia (Ramon y Cajal, 1911; Schmechel and Rakic, 1979; Voigt 1989; Juliano *et al.*, 1996). During development, some of these cells migrate toward the cortex. As the

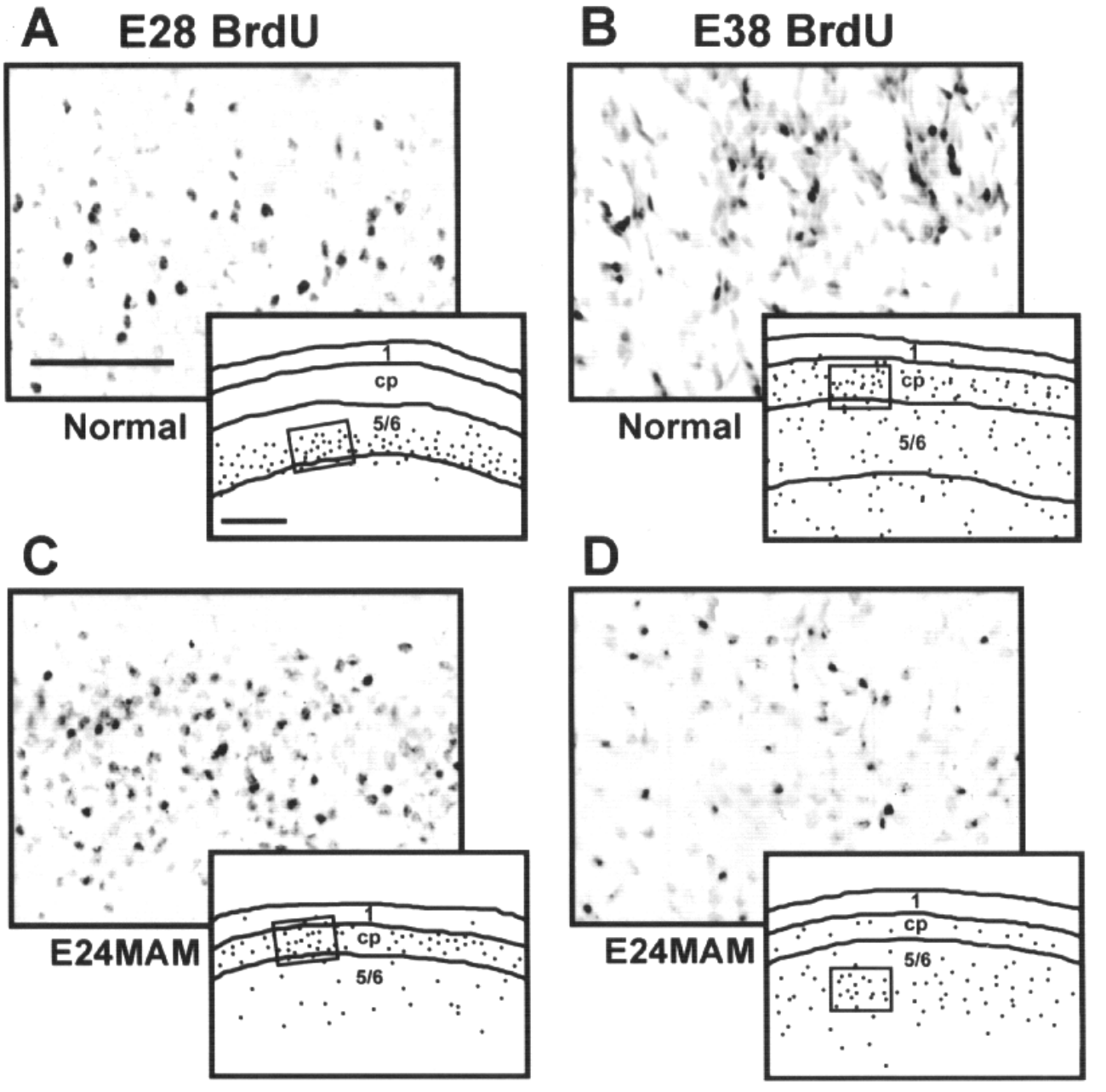

Figure 6. Photomicrographs of BRDU-labeled cells in the positions indicated by the boxes in the inset drawings. Shown are the distribution of BRDU-positive cells in normal and E24 MAM-treated animals at P0 after BRDU injection at E28 (left panels) or E38 (right panels). In a normal animal after E28 BRDU administration the labeled cells reside in a distinct band corresponding to layers 5 and 6, while in E24 MAM-treated animals the BRDU cells are scattered throughout the cortical thickness. After E38 BRDU injections, the cells generated on that day have not yet reached their final position on P0 (birth occurs after 41–42 days of gestation in the ferret) but are distributed throughout the cortical thickness in normal animals. In the E24 MAM-treated animal, cells are also scattered throughout the thin cortical plate and in the ventricular zone.

cortex matures, radial glia transform into astrocytes, which populate the adult cerebral cortex (Schmechel and Rakic, 1979; Levitt and Rakic, 1980, Voigt, 1989, Culican *et al.*, 1990; Raff, 1989). To study the effect of MAM treatment on these cells, we incubated sections of ferret brains with antibodies directed against vimentin, which is an intermediate filament protein established as a marker for radial glia in developing ferret brain (Voigt, 1989). The normal pattern of vimentin immunoreactivity can be seen in Figure 10A; in neonatal ferrets the distribution consists of elongated fibers that extend from the VZ to the pia. The pattern of vimentin immunoreactivity assessed in animals treated with MAM on E33 appears relatively normal, also comprised of elongated fibers that extend from the VZ to pia (Fig. 10*B*). After MAM treatment on E24 or E28, however, the distribution of vimentin immunoreactivity was distorted; the precise radial pattern of staining disappears, revealing stained fibers that are not aligned in radial arrays (Fig. 10*C*). This pattern of vimentin immunoreactivity is similar to that seen in Figure 3*E*,*F*, after dextran injections into the IZ region of acute slices. The immunoreactivity in this region (i.e. as in Fig. 10*C*) reveals fragments of radial glia that remain, or presumptive astrocytes that have formed early. We believe that the immunoreactive pattern demonstrates a relative transitional state, with remnants of radial glia plus the presence of new astrocytes. In normal

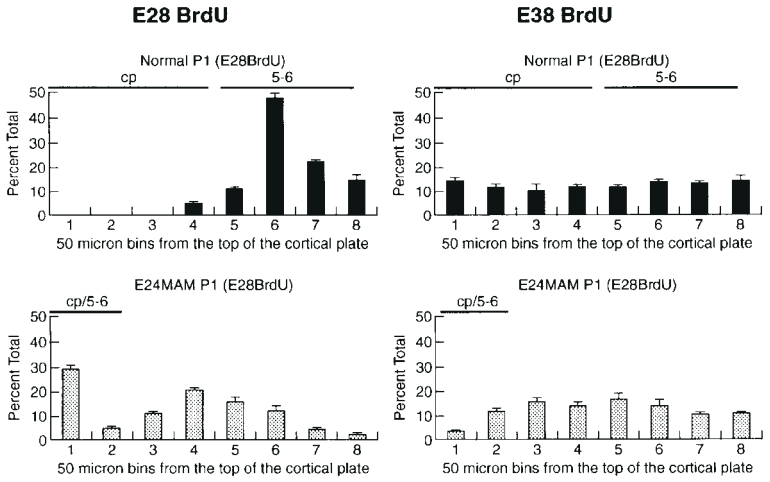

Figure 7. These histograms display the relative percentages of BRDU-positive cells found in the somatosensory cortex after BRDU injections on E28 or E38 in normal and E24 MAM-treated animals. Each bar represents the relative percentage of labeled cells counted in a bin 500 μm wide and 50 μm deep. The cells were counted in bins extending from the pia to a depth of 400 μm. The top two panels show that in normal animals the greatest percentage of cells generated on E28 are in layer 5 on P0, whereas after E38 injections the cells incorporating BRDU have not yet reached their final layer by P0. In the E24 MAM-treated animals, the greatest percentage of counted cells reach the cortical plate after an E28 injection, whereas after an E38 injection many fewer cells reach the cortical plate, but are scattered through the intermediate zone in the E24 MAM-treated animal.

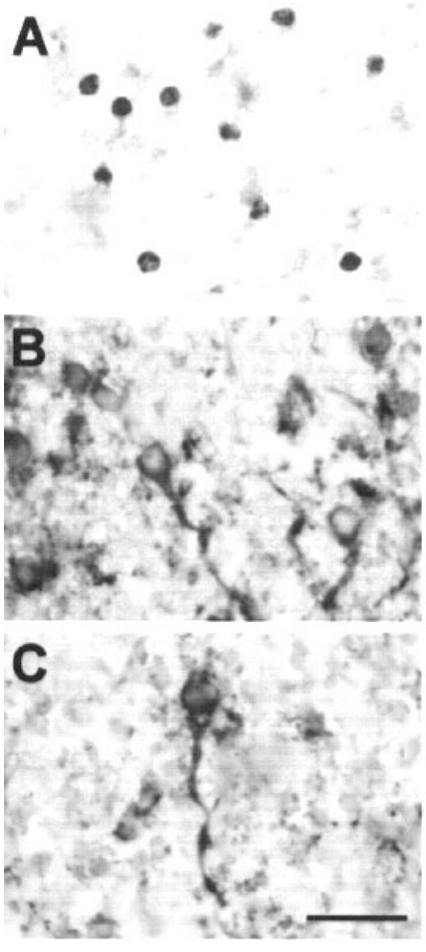

Figure 8. (*A*) A photomicrograph of BRDU-labeled cells found in the subplate, taken from the region indicated by the rectangle in Figure 2*A*, of a normal animal injected with BRDU on E24; subplate cells that populate ferret somatosensory cortex are born over several days, including E24. (*B*) An image of MAP2 immunoreactivity taken from the same region in a normal animal. (*C*) An image of MAP2 immunoreactivity taken from a P0 ferret treated with MAM on E24 in the region indicated by the rectangle in Figure 2*C*. Scale = 50 μm.

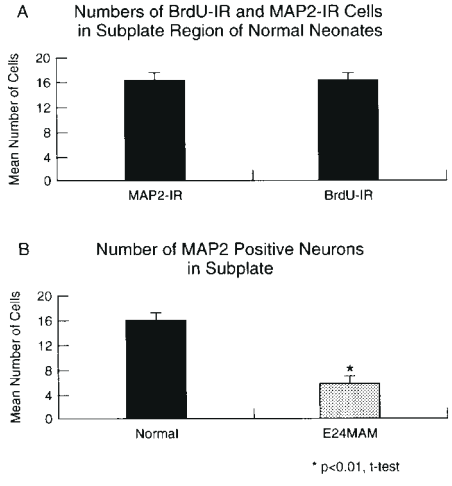

Figure 9. Histograms representing the number of MAP2-positive or BRDU-positive cells in the subplate region of normal and E24 MAM-treated P0 ferrets. (*A*) demonstrates that the mean number of BRDU-positive cells (after labeling on E24) is similar to the mean number of MAP2-positive cells. A mean of 15.1 (SE 0.82) BRDU-IR cells and 16.13 (SE 1.38) MAP2-IR cells were found; there were three animals in each group (two-sample *t*-test, $P = 0.48$). (*B*) demonstrates that the mean number of MAP2-IR neurons in the subplate was reduced in the E24 MAM-treated cortex, a mean of 16.13 (SE 1.38) cells were found in the normal animals and a mean of 5.67 (SE 0.63) cells in the E24 MAM-treated animals; three animals per group. There was a significant difference between the number of MAP2-IR cells in the normal animals and the number of MAP2-IR cells in the subplate region of the E24 MAM-treated animals (two-sample *t*-test, $P < 0.004$).

ferrets, there is little cross-reactivity between GFAP and vimentin immunoreactivity, except during a transitional period at ~2 weeks of age (e.g. Figure 11; Voigt, 1989).

In the majority of locations observed in the E24 MAM-treated animals, the pattern of vimentin immunoreactivity was similar to that displayed in Figure 10*C* or Figure 3*E*,*F*; however, in the most lateral regions of cortex, the staining pattern was more radial in orientation and similar to the normal arrangement. This lateral region is not shown, since it is not a focus of this study (i.e. outside of the region designated in Fig. 1). It is not surprising, however, that lateral regions of neocortex display a relatively

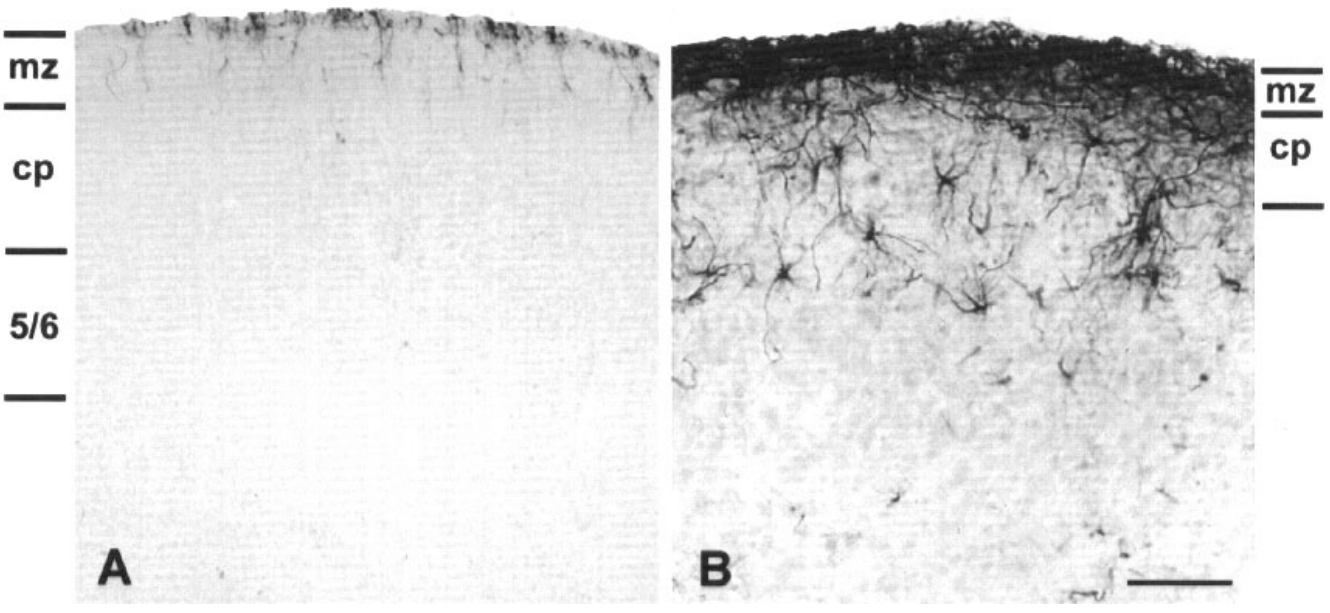

Figure 11. GFAP immunoreactivity on P0 in sections taken from normal (*A*) and E24 MAM-treated ferrets (*B*). In the normal somatosensory cortex, small amounts of anti-GFAP staining can be observed in the outer part of layer 1, near the pial surface. In the E24 MAM-treated brain, many immunoreactive cells that appear morphologically similar to astrocytes are observed scattered through the cortical thickness and intermediate zone. Scale = 100 μm.

astrocytes) throughout the thickness of the cortex and IZ, which appear comparable in overall distribution to the vimentin immunoreactivity in similar animals (Fig. 11*B*).

To further verify the presence of GFAP in E24 MAM-treated kits, Western blots were prepared on tissue obtained from normal and E24 MAM-treated brains at P0. The samples were taken from the designated region of the parietal cortex and underlying white matter in the VZ. These data are presented in Figure 12, and demonstrate that although small amounts of GFAP are present in normal P0 ferret brains, the MAM-treated brains contain substantially greater amounts of this protein. Two bands immunoreactive for GFAP were observed, one at 55 kDa and one at 49 kDa. This was not unusual compared to previous studies, and is likely to be a result of degradation of the molecule (Bigbee *et al.*, 1983; Sheng *et al.*, 1994).

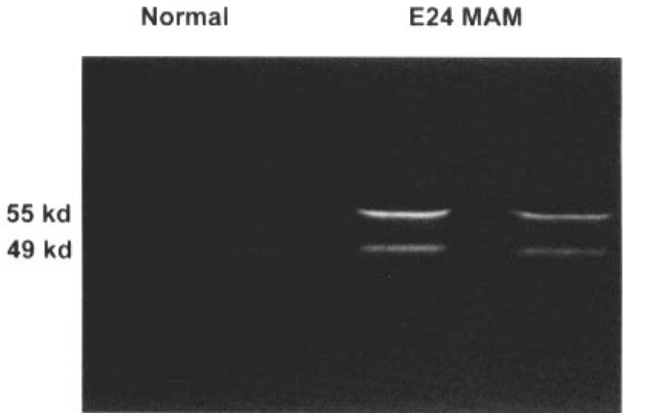

Figure 12. Western blot of normal and E24 MAM-treated brains at P0 demonstrating the presence of GFAP (mol. wt 55 and 49 kDa); two immunoreactive bands are often found in Western blots identifying GFAP. Substantially more GFAP is present in the E24 MAM-treated brain; two different dilutions are shown with the strongest concentrations for both the normal and E24 MAM-treated animals in the center. The weaker concentrations (by 10×) are on the extreme right and the extreme left. Numbers on the left indicate the mol. wt of the standards run with the gel.

Layer 1/Cajal–Retzius Cells

Another component of early-generated cortex are the Cajal–Retzius cells, which populate layer 1. These cells also originate early during development and may have been affected by MAM treatment early during corticogenesis. To assess the presence and distribution of Cajal-Retzius cells, we used the CR50 antibody, which was generated against reelin (Ogawa *et al.*, 1995; D'Arcangelo *et al.*, 1997). Evaluation of normal and E33 MAM-treated sections taken from P0 parietal cortex reveals that CR50 immunoreactivity is restricted to layer 1. The labeled cells have an elongated, horizontal morphology and appear similar in shape and distribution to previous reports of Cajal–Retzius cells (Fig. 13*A*,*C*; e.g. Ramon y Cajal, 1911; Derer and Derer, 1990; Frotscher, 1997; Marin-Padilla, 1998). In P0 sections taken from animals treated with MAM on E24, however, the distribution of CR50-IR cells was dramatically disorganized. Rather than being horizontally positioned in the outer portion of layer 1, the cells were dispersed throughout the thickness of the cortical plate in a wide range of orientations, and extended into the IZ (Fig. 13*B*,*D*). Although the distribution of CR50-positive cells in E24 MAM-treated animals was consistently disorganized, there was variation in the number of displaced cells and in whether they were located in relative superficial positions (i.e. in or near layer 1) or more deeply, extending into the IZ (Fig. 14). Furthermore, we found that the relationship between the disorganization of CR50-IR cells and the thickness of layer 1 was inversely correlated. Therefore the CR50-IR cells were more disorganized and deeply located in sites where layer 1 was very thin; they were more superficially located, although somewhat disorganized, in sites where layer 1 was thicker (Figure 14). Inspection of the sections in the E24 MAM-treated animals indicated that the CR50-IR cells appeared to occur in a greater density. To assess this possibility we counted the CR50-IR cells in a defined region of normal and E24 MAM-treated brains. Within a defined region of neocortex (see Materials and Methods), there are approximately the same numbers of CR50-IR cells in normal (n = 1593.6) and E24 MAM-treated brains (n = 1618.2). Because the E24 MAM-treated brains are substantially smaller than normal brains, more cells distribute over a smaller area, although approximately the same number of cells are present.

Time Course

To help determine the time course of events in the abnormal vimentin and GFAP immunoreactivity, MAM was injected on E24 and the embryos removed by cesarean section on E27 or E35, for one set of kits each. The E27 time point allowed a relatively short interval between the administration of MAM and the assessment of radial glial morphology, as revealed by staining with antibodies directed against vimentin. On E27, the pattern of immunoreactivity appeared similar to that seen in both the normal and E33 MAM-treated animals, but somewhat sparser (Fig. 15). Although the pattern of staining was sparser than that seen in normal P0 animals and fetuses at later embryonic dates (e.g. E38), the stained processes were distinctly radial and extended from the VZ to the pial surface. Nissl stains of this material demonstrated that the elements of the cortical plate formed by E27 appeared relatively normal. At this time point, although very thin, there was no obvious disruption of the cortical plate; layer 1 was present and contained cells, including presumptive neurons. In kits studied at E35 after E24 MAM treatment, vimentin immunoreactivity was distorted and the radial glia were not aligned in their normal radial pattern.

Discussion

Effects of MAM Treatment on Overall Cortical Organization and Laminar Pattern

MAM has been used by a number of researchers to interfere with the development of a specific neocortical layer or layers. These and the present study indicate that MAM treatment is relatively discrete, and acts for a restricted window of time (Kind *et al.*,1992; Woo and Finley, 1996; Woo *et al.*, 1996; Cattabeni and Di Luca, 1997). In our study, the differences between injections of MAM at early and mid-gestational points during cortical neogenesis are dramatic. Later injections (E33) result in a relatively distinct disruption of layer-specific development (Kind *et al.*,1992; Woo *et al.*, 1996). Subsequent injections of BRDU indicate that cells continue to be generated and migrate into the cortex in a layer-specific manner after MAM treatment. Although there may be effects on later generated cells, these are not evident. Early MAM injections, however, severely disturb the formation of cortical layers and result in distorted radial glial cells. Injections of MAM early during cortical genesis almost certainly interfere with the division of precursor cells as well as cells undergoing their final division at the time of injection, which could contribute to a poorly formed laminar pattern. We cannot rule out that the thin and disarrayed cortical plate after

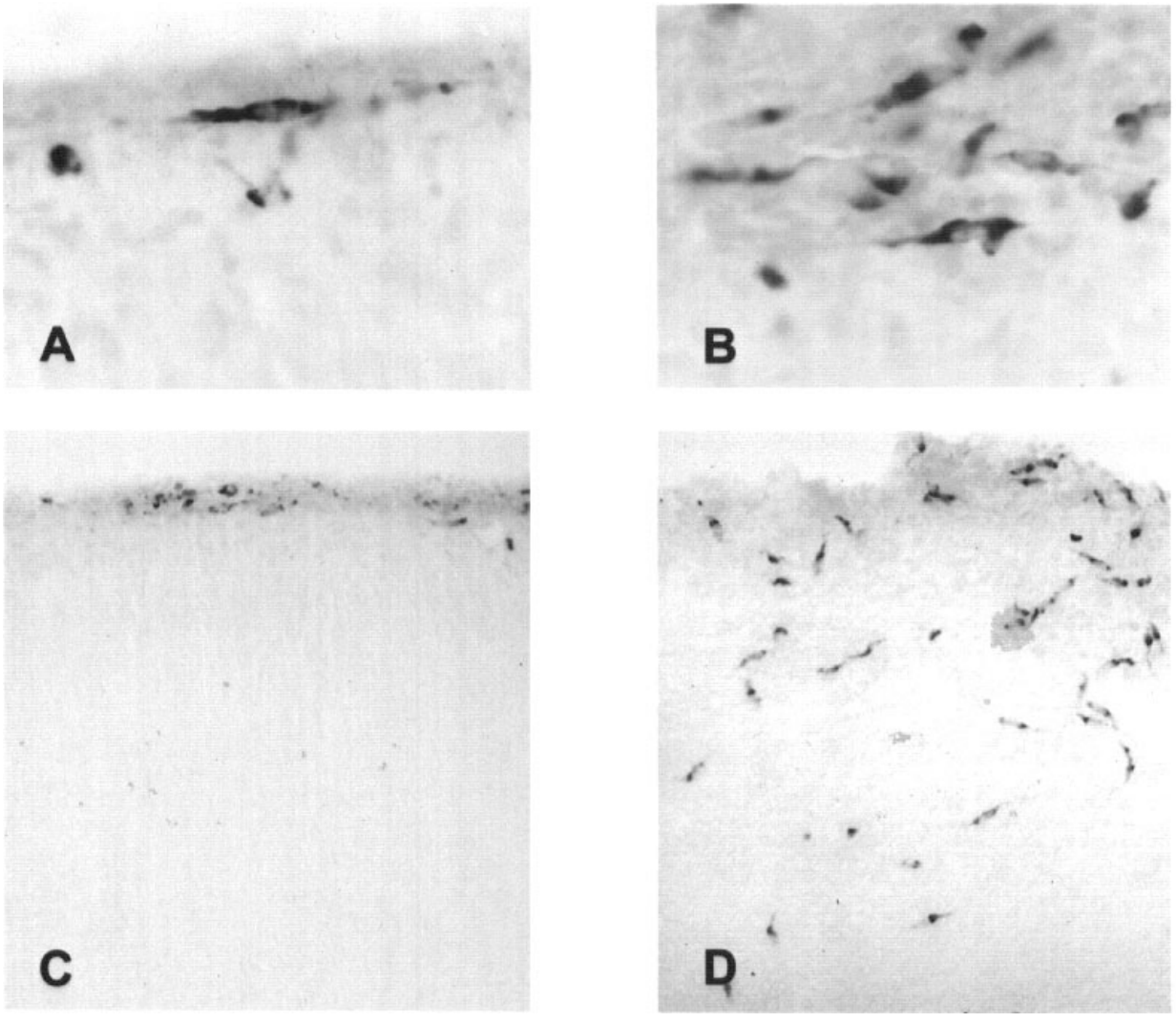

Figure 13. Examples of immunoreactivity against the CR50 antibody demonstrating presumptive Cajal–Retzius cells in normal (*A*,*C*) and E24 MAM-treated (*B*,*D*) P1 cortex. In the normal animals (*A*,*C*) immunoreactivity is restricted to layer 1, the presumptive Cajal–Retzius cells display the horizontal morphology typical of these neurons. In the MAM-treated animals (*B*,*D*), the IR cells are distributed throughout the cortical plate and the intermediate zone, although they continue to display the usual horizontal morphology.

early MAM treatment is partially due to eliminating a portion of precursor cells that are substrates for subsequently born cells. Cells continue to be born and migrate into the cortical plate, however, after early MAM treatment. BRDU is incorporated into dividing cells at several time points after the MAM injection (e.g. Figs 7, 8) suggesting that auxiliary mechanisms contribute to the jumbled cortical pattern in addition to a possible reduction in cortical precursors.

We believe that the data presented here support the idea that MAM eliminates a cohort of cells generated at the time of injection, i.e. E24 or E33. This treatment leads to relatively minor architectural changes after the E33 injection and relatively major structural and histochemical changes after the E24 injection. The mechanism of action of MAM has been well described and, as indicated above, several other investigators find that MAM interferes with the generation of neocortical layers by eliminating a specific population of cells. There remains the possibility that the administration of MAM acts in some other (i.e. toxic) way that alters cellular function, leading to the findings reported here. Several studies identify MAM as a carcinogen, but those experiments have used either dosages much higher than those used here, or multiple doses (Zedeck and Swislocki, 1975; Zedeck and Brown, 1977). Our interpretation is also supported by the observation that MAM injections during later stages of corticogenesis (E33) do not result in any of the changes observed in radial glia or Cajal–Retzius cells.

MAM treatment may also interfere with the development of other neural centers that influence the neocortex, most notably the thalamus. Although we cannot completely discount the possibility that an alteration in thalamocortical projection influenced the development of cortical layering, in ongoing parallel studies we find a strong projection from the thalamus to the neocortex in similar E24 MAM-treated animals (Palmer *et al.*, 1997). In addition, Algan and Rakic (1997) using a different model of cell cycle disruption, ionizing radiation, found that delivering doses of X-rays during the development of the lateral geniculate nucleus does not substantially reduce the thickness of the visual cortex or the overall laminar pattern, suggesting that these particular features are not dramatically altered by reduced input from the thalamus. This treatment does, however, reduce the total surface devoted to area 17.

Our analysis of MAP2-positive cells in the subplate region

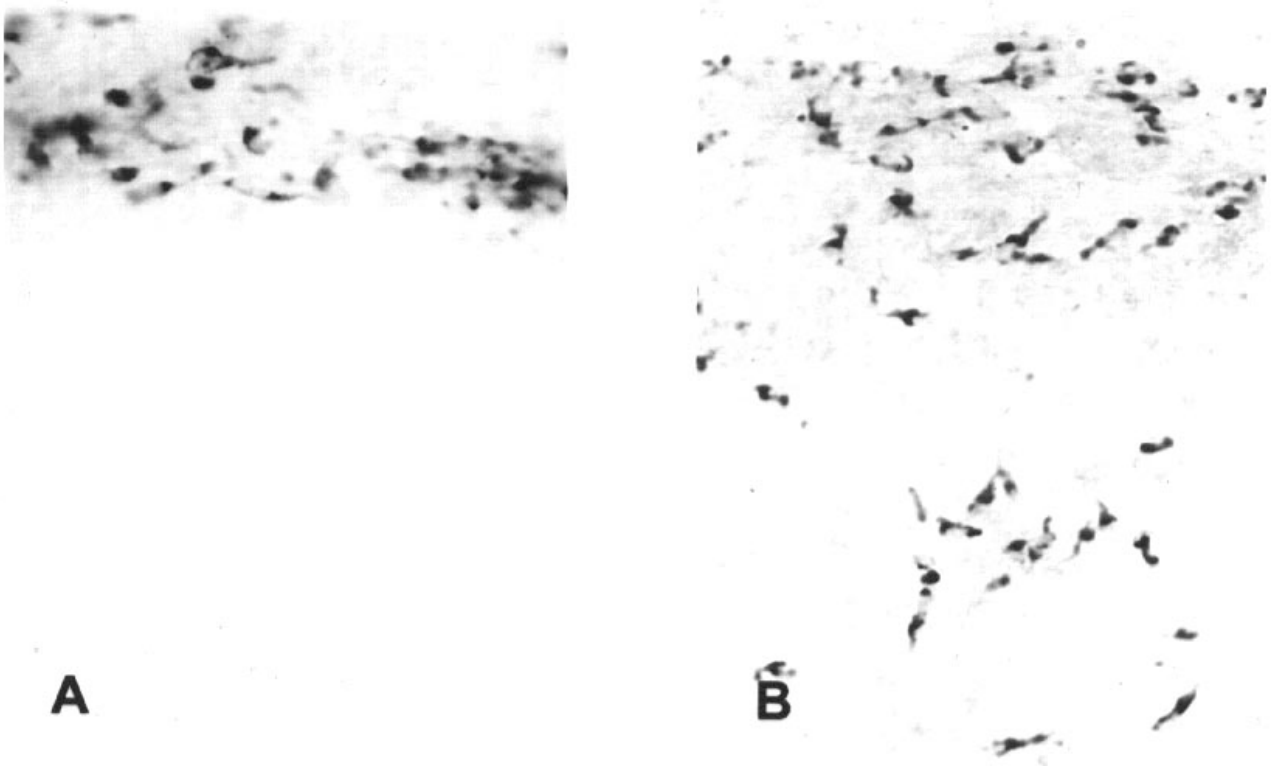

Figure 14. Immunoreactivity against the CR50 antibody in sections taken from E24 MAM-treated animals on P1. Illustrated are examples of presumptive Cajal–Retzius cells that display immunoreactivity either clustered in the vicinity of layer 1 (*A*), or scattered throughout the cortical plate and intermediate zone (*B*). When CR50-positive cells occurred near layer 1, they generally correlated with a more normal appearing layer 1; when the CR50-positive cells were distributed throughout the cortical plate and intermediate zone, layer 1 was very thin.

finds that the number of MAP2-IR cells are drastically reduced in the animals treated with MAM on E24 compared to normal animals. This analysis was confined to the subplate region and it is possible that cells technically belonging to the subplate may be elsewhere, ectopically placed. Theoretically, subplate neurons may be generated before or after the MAM injection, since subplate neurons that populate somatosensory cortex are born over a period of several days (Noctor *et al.*, 1997) and could be found in the subplate region, or may be located in other sites because of a failure to migrate properly. The likelihood that ectopically placed neurons are present is confirmed by our BRDU data (Figs 6, 7), which show that in the E24 MAM-treated animals a greater percentage of BRDU-positive cells are found in the IZ than in normal animals. The BRDU-positive cells identified in Figures 6 and 7 are not subplate neurons since they are BRDU-labeled on dates after the MAM injection and after the birth of the subplate. Even if we counted ectopically placed MAP2 neurons, we could not be sure if they were cells intended for the subplate or other layers. The counting of MAP2-positive cells that we accomplished in Figure 9 demonstrates that cells intended for the subplate have not made it to that site; it is possible that a few subplate cells were born and have located elsewhere, i.e. in the IZ or cortical plate. Probably, many subplate cells are eliminated by the MAM treatment, and some get 'lost' in the IZ or are inappropriately located in the cortical plate.

Shortly after early MAM injection (on E27 after E24 injection) both the radial glia and cortical plate look relatively normal. This suggests that the process of disorganization does not begin immediately, but takes place over a period of some days. In addition, injections of BRDU at different dates after early MAM

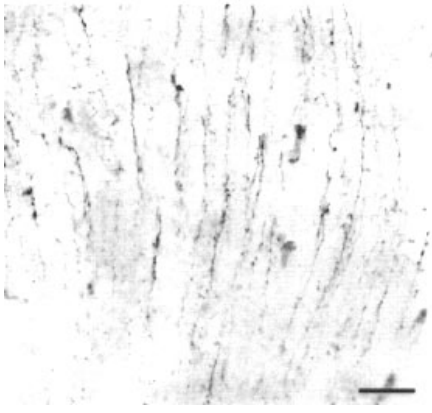

Figure 15. Immunoreactivity against vimentin in a section taken from an E27 embryo that was previously treated with MAM on E24. At this age after MAM treatment, the radial glia are present and organized similar to their distribution in normal P0 kits, but the distribution is sparse.

treatment indicate that neurons continue to be born and make their way to the cortical plate. In fact, 4 days after (E28) the early MAM injection, BRDU injections reveal that cells continue to be born and migrate into cortex in numbers at least equal to the normal animal. They form a quasi-laminar pattern, with the greatest percentage of cells born on that day reaching the cortex (Figs 6, 7). BRDU injections at a later time (E38) after early MAM injection, show that cells continue to be born, but fewer are found in the cortical plate at P0. Even in the normal animal at this age the migrating cells have not clearly attained their discrete

laminar arrangement and maintain a substantial presence in the IZ. They would normally reside in layer 2 if further development and migration were permitted. Since the disrupted pattern of radial glia takes place gradually after E24 MAM treatment, the earlier born neurons may travel into cortex more easily than those generated later.

Effects of MAM Treatment on Radial Glia

One of the more dramatic features of early MAM injections is the disorganized radial glia. Our interpretation that radial glia are disorganized after early MAM treatment is supported by observations that include lack of radial organization in the IZ after dextran injections in acute slices, absence of a normal pattern of vimentin immunoreactivity, and a substantial increase in GFAP immunoreactivity (demonstrated immunohistochemically and with Western blots). Why would early MAM injections result in a distorted distribution of radial glia, while the late MAM injections have no effect on these cells? It is generally assumed that radial glia are generated early in cortical development and are present when neurons that populate the cerebral cortex are born (Schmechel and Rakic, 1979; Altman and Bayer, 1991). They then provide, at least partially, a scaffold for neurons to reach the neocortex (Rakic, 1971, 1972, 1977, 1990, 1995). This idea seems to be validated by the current study, since several days after early MAM injection at E24, the radial glia are present and relatively intact. The radial glia are apparently in place at the time of MAM injection at E24; the process of radial glial distortion takes place over a period of several days, supported by our observation that 3 days after injection the cortical structure appears relatively normal, but by birth is highly abnormal in appearance. MAM treatment alone does not seem to cause specific distortion or death of radial glia, since later injections do not result in radial glial malformation (e.g. injections on E33). Therefore a specific aspect of interfering with early, but not later, developing cortex results in this process. The observation that early injections of MAM result in radial glial distortion also argues against the idea that disruption of radial glia is due to reactive gliosis. If the glial distortion was due to reactive gliosis, as a result of MAM injection alone, one would expect this finding after later injections of MAM as well. We cannot entirely eliminate the possibility, however, that other undetected effects of MAM treatment may occur that influence neural development.

It seems highly likely that the radial glia are differentiating into astrocytes earlier than normal. It is widely accepted that many radial glia become astrocytes after they are no longer necessary as guides for neurons traveling to the neocortex (Schmechel and Rakic, 1979; Raff, 1989; Voigt, 1989, Culican *et al.*, 1990). Our demonstration of a change in morphology, plus increased expression of the characteristic marker for astrocytes, GFAP, strongly suggests that the radial glia of early MAM-treated animals differentiate into astrocytes. If this is the case, several mechanisms might contribute to this conversion. Early interruption of the generation of cortical cells will block (at least partially) the formation of the cortical layers produced first, including the subplate. It is not clear which comes first: the failure of layers to form or the disruption of radial glia. One possibility is that the lack of a feature normally supplied by the early generated neocortex causes the radial glia to differentiate into astrocytes. The subplate is a substantial component of the early generated neocortex and contains many cell adhesion and extracellular matrix molecules that are not present in other parts of the developing cortical plate (see Allendoerfer and Shatz, 1994, for review). These molecules may be important for maintenance of radial glial attachment, as well as for axonal guidance or other growth processes. Interestingly, Hunter and Hatten (1995) demonstrated that a diffusable factor present in mouse embryonic neocortex induces astrocytes to alter their cell phenotype into radial glia-like. They suggest an inhibitory factor may be present during cortical neogenesis and layer formation, which maintains radial glia in their proper morphology. With cortical maturity, this factor is withdrawn and radial glia are free to differentiate into astrocytes. It is possible that in our study, the early MAM treatment induces withdrawal of the normally present inhibition resulting in early formation of astrocytes. The subplate, with its high complement of trophic substances may be a source for the factor causing radial glia differentiation. In normal ferrets, transformation of radial glia into astrocytes is coincident with the developmental period in which subplate neurons disappear from the cortex (Voigt, 1989; Allendoerfer and Shatz, 1994; Juliano *et al.*, 1996). Although our study of E27 embryos after E24 MAM treatment suggests that the cortical layers begin to form normally after MAM treatment, perhaps after transformation of the radial glial guides, newly generated cortical neurons cannot find their way to the cortex, leading to the severely disrupted cortical pattern we observed. A recent study by Hunter-Schaedle (1997) reports that radial glia in the *reeler* mouse are also disrupted and display early differentiation into astrocytes. She suggests that poorly developed radial glia may participate in the disturbed formation of layers in the *reeler* neocortex.

Involvement of Layer 1 and Cajal–Retzius Cells

Abnormal radial glia may also be induced due to an incomplete formation of the preplate at the time of early MAM injection. During early cortical genesis, the first generated component of the neocortex is the preplate, which consists of the marginal zone (future layer 1) and the subplate (which largely dies in the adult). As cortical neurons are generated, the preplate splits into a superficial marginal zone and a deeper subplate to allow neurons of the cortical layers to insinuate themselves in between the two preplate layers. If early MAM treatment interferes with normal marginal zone formation, a usual substrate for radial glia would not be intact and might cause early astrocytic differentiation. The results presented here indicate that although layer 1 is present after early MAM treatment, it varies in thickness and an important cellular component of this layer is highly distorted. We found that the cells identified by CR50-IR cells (presumptive Cajal–Retzius cells) were not in their normal position in layer 1, but in disarray throughout the thickness of the cortical plate and into the IZ. Many researchers suggest that layer 1, and particularly the Cajal–Retzius neurons, play an important role in attracting and guiding subsequent neurons to their proper positions (e.g. Caviness and Rakic, 1978; Marin-Padilla, 1984, 1998; Ogawa *et al.*, 1995). Several lines of evidence suggest that Cajal–Retzius cells provide an environment that acts as a stop signal both for neurons migrating into the neocortex and axons growing into the cortex (Hirotsune *et al.*, 1995; Ogawa *et al.*, 1995; Del Rio *et al.*, 1997; Frotscher, 1997; Marin-Padilla, 1998). In our study, the CR50-IR cells were disorganized and may further contribute to the poorly formed cortex after E24 MAM treatment. If the CR50-positive cells act as a stop signal, misplaced layer 1 neurons may induce migrating cells to 'stop' before they enter the cortical plate. Furthermore, a recent study by Soriano *et al.* (1997) reports that Cajal–Retzius cells strongly influence the phenotype of radial glia in adult and developing cerebellum.

We do not know the mechanism contributing to the dispersed CR50-IR cells. Two scenarios seem possible: (i) distortion of the radial glial cells contributes to, or causes, the CR50-IR cell dispersion or (ii) the presumptive Cajal–Retzius cells are generated after the radial glial disruption and migrate to inappropriate positions without appropriate radial glial guides. Without further experiments, it is difficult to distinguish between these two possibilities, but available evidence strongly suggests that layer 1 Cajal–Retzius cells and radial glial cells are among the earliest generated components of neocortex and are probably already present during most of corticoneogenesis including the time of MAM injections. Since there are roughly the same number of CR50-positive cells in normal and E24 MAM-treated brains, it is likely that they exist at the time of the MAM injection and become distorted after further development. In addition, our earlier study, which determined the birth dates of neurons populating ferret parietal cortex, suggested that layer 1 cells are born prior to E24 (Noctor *et al.*, 1997). It is probable, although hypothetical, that the disruption of radial glia and presumptive Cajal–Retzius cells occur together and the distortion of both elements reinforces the inability of the cortical plate to form properly in the E24 MAM-treated animals.

Relation to Reeler and Other Mouse Mutants

The effects of E24 MAM treatment are clearly not identical to those of the *reeler* mutant mouse, although there are some similarities. The cortical layers fail to form properly in both models. In both animals there is a disruption of reelin, although the mechanism is obviously different in the two animals. In the reeler mutant, the gene encoding reelin is absent, and this protein is not manufactured. In the E24 MAM-treated animal, reelin is present, as revealed by the CR50 antibody, but in inappropriate loci. The *scrambler* mutant, which also displays a disrupted laminar pattern, appears to have normal distribution of reelin, although the reeler gene pathway may be involved in the inverted cortical pattern (Gonzalez *et al.*, 1997). These results imply that reelin is likely to be involved in guiding neuronal migration into the neocortex, as others have suggested. In addition, evidence from the *reeler* mouse mutation suggests that a specific feature of the preplate is important for subsequent formation of neocortex. Although in *reeler* the preplate fails to split and cortical layers pile up underneath the superficial structure (Caviness and Sidman, 1973), the presence of the preplate itself is consequential to several features of subsequent cortical development. In this model, thalamocortical afferents first touch the subplate before turning and terminating in layer 4, suggesting that the preplate itself is an important feature for cortical development (Frost and Caviness, 1980). If the formation of this region is disrupted after early MAM treatment, it may also contribute to the malformation of cortical layers and radial glia by removing a necessary component of proper cortical development.

Summary

These results are consistent with the idea that early generated cortex is necessary for proper laminar formation in the neocortex. The early generated layers may provide cues to the radial glia about where to maintain their processes and when to differentiate into astrocytes. Without the substrate normally provided by the first born layers of neocortex, the radial glia lose their spoke-like orientation and begin astrocytic differentiation. Concomitant with the radial glial distortion, presumptive Cajal–Retzius cells become displaced, and further contribute to the malformed cortex.

Notes

The authors thank Anirvan Ghosh for helpful discussions on this work. These studies were supported by PHS RO1NS24014 (S.L.J.).

Address correspondence to Sharon L. Juliano, Department of Anatomy & Cell Biology, USUHS, 4301 Jones Bridge Road, Bethesda, MD 20814, USA. Email sjuliano@usuhs.mil.

References

Abercrombie M (1949) Estimation of the nuclear population from microtome sections. Anat Rec 94:239–247.

Algan O, Rakic P (1997) Radiation induced, lamina-specific deletion of neurons in the primate visual cortex. J Comp Neurol 381:335–352.

Allendoerfer KL, Shatz CJ (1994) The subplate, a transient neocortical structure: its role in the development of connections between thalamus and cortex. Annu Rev Neurosci 17:185–218.

Altman SA, Bayer J (1991) Neocortical development. New York: Raven Press.

Antonini A, Shatz CJ (1990) Relation between putative transmitter phenotypes and connectivity of subplate neurons during cerebral cortical development. Eur J Neurosci 744–761.

Bigbee JW, Bigner DD, Pegram C, Eng LF (1983) Study of glial fibrillary acidic protein in a human glioma cell line grown in culture and as a solid tumor. J Neurochem 460–467.

Blanton MG, Lo Turco JJ, Kriegstein AR (1989) Whole cell recording from neurons in slices of reptilian and mammalian cerebral cortex. J Neurosci Methods 30:203–210.

Calloway EM (1998) Prenatal development of layer-specific local circuits in primary visual cortex of the Macaque monkey. J Neurosci 18:1505–1527.

Cattabeni F, Di Luca M (1997) Developmental models of brain dysfunctions induced by targeted cellular ablations with methyl-azoxymethanol. Physiol Rev 77:199–214.

Caviness VS, Frost DO (1983) Thalamocortical projections in the Reeler mutant mouse. J Comp Neurol 219:182–202.

Caviness VS, Jr, Rakic P (1978) Mechanisms of cortical development: a view from mutations in mice. Annu Rev Neurosci 1:297–326.

Caviness VS, Jr, Sidman RL (1973) Time of origin of corresponding cell classes in the cerebral cortex of normal and reeler mutant mice: an autoradiographic analysis. J Comp Neurol 148:141–152.

Culican SM, Baumrind NL, Yamamoto M, Pearlman AL (1990) Cortical radial glia: identification in tissue culture and evidence for their transformation to astrocytes. J Neurosci 10:684–692.

D'Arcangelo G, Nakajima K, Miyata, T, Ogawa M, Mikoshiba K, Curran T (1997) Reelin in a secreted glycoprotein recognized by the CR-50 monoclonal antibody. J Neurosci 17:23–31.

De Carlos JA, O'Leary DDM (1992) Growth and targeting of subplate axons and establishment of major cortical pathways. J Neurosci 12:1194–1211.

Del Rio JA, Heinrich B, Borrel V, Forster E, Drakew A, Alcantara S, Nakajima K, Miyata T, Ogawa M, Mikoshiba K, Derer P, Frotscher M, Soriano E 1997A role for Cajal–Retzius cells and reelin in the development of hippocampal connections. Nature 385:70–74.

Derer P, Derer M (1990) Cajal–Retzius cell ontogenesis and death in the mouse brain visualized with horseradish peroxidase and electron microscopy. Neuroscience 36:839–856.

Erzurumlu RS, Jhaveri S (1992) Emergence of connectivity in the embryonic rat parietal cortex. CerebCortex 2:336–352.

Fasolo A, Virgili M, Panzica GC, Constestabile A (1992) Immuno-histochemistry and neurochemistry of the habenulo-interpeduncular connection after partial developmental depletion of habenular cholinergic neurons in the rat. Exp Brain Res 90:297–301.

Flint AC, Maisch US, Weishaupt J, Monyer H, Kriegstein AR (1997) NR2A subunit expression shortens NMDA receptor synaptic currents in developing neocortex. J Neurosci 17:2469.

Frost DO, Caviness VS (1980) Radial organization of thalamic projections to the neocortex in the mouse. J Comp Neurol 194:369–393.

Frotscher M (1997) Dual role of Cajal–Retzius cells and reelin in cortical development. Cell Tissue Res 290:315–322.

Ghosh A, Shatz CJ (1992a) Involvement of subplate neurons in the formation of ocular dominance columns. Science 255:1441–1443.

Ghosh A, Shatz CJ (1992b) Pathfinding and target selection by developing geniculocortical axons. J Neurosci 12:39–55.

Ghosh A, Shatz CJ ((1993)) A role for subplate neurons in the patterning

of connections from thalamus to neocortex. Development 117: 1031–1047.
Ghosh A, Shatz CJ (1994) Segregation of geniculocortical afferents during the critical period: a role for subplate neurons. J Neurosci 14:3862–3880.
Ghosh A, Antonini A, McConnell SK, Shatz CJ (1990) Requirement for subplate neurons in the formation of thalamocortical connections. Nature 347:179–181.
Gonzalez JL, Russo CJ, Goldowitz D, Sweet HO, Davisson MT, Walsh CA (1997) Birthdate and cell marker analysis of scrambler: a novel mutation affecting cortical development with a reeler-like phenotype. J Neurosci 17:9401–9411.
Guillery RW, Herrup K (1997) Quantification without pontification: choosing a method for counting objects in sectioned tissues. J Comp Neurol 386:2–7.
Hirotsune S, Takahare T, Sasaki N, Hirose K, Yoshiki A, Ohashi T, Kusakabe M, Murakami Y, Muramatsu M, Watanabe S, Nakao K, Katsuki M, Hayashizaki Y (1995) The reeler gene encodes a protein with an EGF-like motif expressed by pioneer neurons. Nat Genet 10:77–83.
Hunter KE, Hatten ME (1995) Radial glial cell transformation to astrocytes is bidirectional: regulation by a diffusable factor in embryonic forebrain. Proc Natl Acad Sci USA 92:2061–2065.
Hunter-Schaedle KE (1997) Radial glial development and transformation are disturbed in reeler forebrain. J Neurobiol 33:459–472.
Johnston MV, Coyle JT (1979) Histological and neurochemical effects of fetal treatment with methylazoxymethanol on rat neocortex in adulthood. Brain Res 170:135–155.
Johnston MV, Grzanna R, Coyle JT (1979) Methylazoxymethanol treatment of fetal rats results in abnormally dense noradrenergic innervation of neocortex. Science 203:369–371.
Jones EG, Valentino KL, Fleshman JW (1982) Adjustment of connectivity in rat neocortex after prenatal destruction of precursor cells of layers II–IV. Dev Brain Res 2:425–431.
Juliano SL, Palmer SL, Noctor SC, Sonty R, Hill G (1996) Development of local connections in ferret somatosensory cortex. J Comp Neurol 374:259–277.
Kandler K, Katz LC (1998) Coordination of neuronal activity in developing visual cortex by gap junction-mediated biochemical communication. J Neurosci 18:1419–1427.
Kind P, Sengpiel F, Engelage J, Blakemore C (1992) Interference with generation of layer 4 prevents the formation of ocular dominance columns. Soc Neurosci Abstr 18:1314.
Levitt P, Rakic P (1980) Immunoperoxidase localization of glial fibrillary acidic protein in radial glial cells and astrocytes of the developing rhesus monkey brain. J Comp Neurol 193:815–840.
Luskin MB, Shatz CJ (1985) Studies of the earliest generated cells of the cat's visual cortex: cogeneration of subplate and marginal zones. J Neurosci 5:1062–1075.
Luskin MB, Shatz CJ (1985) Neurogenesis of the cat's primary visual cortex. J Comp Neurol 242:611–631.
Marin-Padilla M (1990) Three dimensional structural organization of layer I of the human cerebral cortex: a golgi study. J Comp Neurol 299:89–105.
Marin-Padilla M (1984) Neurons of layer I: a developmental analysis. In: Cerebral cortex (Peters A, Jones EG, eds), vol. 1. New York: Plenum Press.
Marin-Padilla M (1998) Cajal–Retzius cells and the development of the neocortex. Trends Neurosci 21:64–70.
Matsumoto H, Higa HH (1966) Studies on methylazoxymethanol, the algycone of cycasin: methylation of nucleic acids *in vitro*. Biochem J 98:20C–22C.
Matsumoto H, Spatz M, Laquer GL (1972) Quantitative changes with age in the DNA content of methylazoxymethanol-induced microcephalic rat brain. J Neurochem 19:297–306.
McConnell SK, Ghosh A, Shatz CJ (1989) Subplate neurons pioneer the first axon pathway from the cerebral cortex. Science 245:978–982.
McConnell SK, Ghosh A, Shatz CJ (1994) Subplate pioneers and the formation of descending connections from cerebral cortex. J Neurosci 14:1892–(1907).
McLaughlin DF, Sonty RV, Juliano SL (1998) Organization of the forepaw representation in ferret somatosensory cortex. Somatosens Mot Res 15:253–268.
Misson J-P, Edwards MA, Yamamoto M, Caviness VS, Jr (1988) Identification of radial glial cells within the developing murine central nervous system: studies based upon a new immunohistochemical marker. Dev Brain Res 44:95–108.
Molnar Z, Blakemore C (1995) How do thalamic axons find their way to the cortex? Trends Neurosci 18:389–397.
Noctor SC, Palmer SL, Juliano SL (1995) Effects of methylazoxymethanol (MAM) treatment on development of somatosensory cortex. Soc Neurosci Abstr 21:26.15.
Noctor SC, Scholnicoff NJ, Juliano SL (1997) Histogenesis of ferret somatosensory cortex. J Comp Neurol 387:179–193.
Ogawa M, Miyata T, Nakajima K, Yagyu K, Seike M, Ikenaka K, Yamamoto H, Mikoshiba K (1995) The reeler gene-associated antigen on Cajal–Retzius neurons is a crucial molecule for laminar organization of cortical neurons. Neuron 14:899–912.
Palmer SL, Noctor SC, Juliano SL (1997) Thalamocortical development in normal, E24, and E33 MAM-treated ferret somatosensory cortex. Soc Neurosci Abstr 23:39.10.
Raff M (1989) Glial cell diversification in the rat optic nerve. Science 243:1450–1455.
Rakic P (1971) Guidance of neurons migrating to the fetal monkey neocortex. Brain Res 33:283–312.
Rakic P (1972) Mode of cell migration to the superficial layers of fetal monkey neocortex. J Comp Neurol 145:61–84.
Rakic P (1977) Prenatal development of the visual system in rhesus monkey. Phil Trans R Soc Lond B 278:245–260.
Rakic P (1990) Principles of neural cell migration. Experientia 46:882–891.
Rakic P (1995) A small step for the cell, a giant leap for mankind: a hypothesis of neocortical expansion during evolution. Trends Neurosci 18:383–388.
Ramon y Cajal S (1911) Histology of the nervous system. Paris: Maloine. Reprinted in translation: Swanson N, Swanson LW (1995) Oxford: Oxford University Press.
Schmechel DE, Rakic P (1979) A Golgi study of radial glial cells in developing monkey telencephalon: morphogenesis and transformation into astrocytes. Anat Embryol 156:115–152.
Sheng JG, Mrak RE, Griffin WST (1994) S100β protein expression in Alzheimer disease: potential role in the pathogenesis of neuritic plaques. J Neurosci Res 39:398–404.
Soriano E, Alvarado-Mallart RM, Dumesnil N, Del Rio JA, Sotelo C (1997) Cajal–Retzius cells regulate the radial glia phenotype in the adult and developing cerebellum and alter granule cell migration. Neuron 18:563–577.
Valverde F, Facal-Valverde MV (1988) Postnatal development of interstitial (subplate) cells in the white matter of the temporal cortex of kittens: a correlated Golgi and electron microscopic study. J Comp Neurol 269:168–(192.)
Virgili M, Barnabei O, Contestabile A (1988) Depletion of cholinergic habenulo-interpeducular neurons by selectively timed methylazoxymethanol acetate (MAM) treatment during pregnancy. Brain Res 460:361–365.
Voigt T (1989) Development of glial cells in the cerebral wall of ferrets: direct tracing of their transformation from radial glia into astrocytes. J Comp Neurol 289:74–88.
Wiser AK, Calloway EM (1996) Contributions of individual layer 6 pyramidal neurons to local circuitry in macaque primary visual cortex. J Neurosci 16:2724–2739.
Woo TU, Finlay BL (1996) Cortical target depletion and ingrowth of geniculocortical axons: implications for cortical specification. Cereb Cortex 6:457–469.
Woo TU, Niederer JK, Finlay BL (1996) Cortical target depletion and the developing lateral geniculate nucleus: implications for trophic dependence. Cereb Cortex 6:446–456.
Yuste R, Nelson DA, Rubin WW, Katz LC (1995) Neuronal domains in developing neocortex: mechanisms of coactivation. Neuron 14:7–17.
Zedeck MS, Brown GB (1977) Methylation of intestinal and hepatic DNA in rats treated with methylazoxymethanol acetate. Cancer 40: 2580–2583.
Zedeck MS, Swislocki NI (1975) Effect of methylazoxymethanol acetate on adenylate cyclase and 5′-nucleotidase in rat liver plasma membranes. Cancer Lett 1:109–112.
Zedeck MS, Sternberg SS, Poynter RW, McGowan J (1970) Biochemical and pathological effects of methylazoxymethanol acetate, a potent carcinogen. Cancer Res 30:801–812.